

CFD ANALYSIS AND CALCULATION OF AERODYNAMIC CHARACTERISTICS OF HELICOPTER ROTOR

N.A. Vladimirova, vlana@progtech.ru,
TsAGI - Central Aerohydrodynamic Institute (Russia)

Abstract

Methods of computational fluid dynamics (CFD) are used to model the flow features and aerodynamic characteristics of helicopter rotor. For the purpose of verification and validation of the numerical methods used, there have been developed the technologies of rotor flow calculations in the two CFD software packages, ANSYS CFX and the new Russian code LOGOS, based on the grid methods of solution of the averaged Navier-Stokes equations (RANS, URANS). The results show good agreement between the 3D calculations of integral and distributed characteristics of rotating two-blade rotor model in hover and the data of experiment carried out by the standard method of TsAGI.

To simulate nonstationary flow characteristics of the various sections of helicopter rotor blades, the technology of 2D calculation of flow about helicopter airfoil with specified periodic law of variation over time of incoming flow velocity in the transonic range has been developed. As a result of numerical investigation of nonstationary flow about NACA 23012 and NACA 0012 airfoils there has been discovered the phenomenon of lift and drag hysteresis against free stream Mach number value. The numerical results obtained are the basis to generate the data bank of stationary and nonstationary aerodynamic characteristics of helicopter airfoils with the use of CFD technologies.

1. NOTATION

D – diameter of the rotor, m
 R – radius of the rotor, m
 r – radius of blade cross section, m
 r_0 – radius of blade root, m
 b – blade chord, m
 k – number of blades
 $\sigma = kb/\pi R$ – filling factor
 n – number of rotor revolutions per minute, min^{-1}
 ω – angular velocity of rotation, rad/s
 φ – angle of incidence of the blade, °
 α – angle of attack, °
 ρ – air density, kg/m^3
 ν – kinematic viscosity of air, m^2/s
 $v = \omega R$ – circumferential velocity of blade end, m/s
 $S = \pi R^2$ – blade-swept area, m^2
 $q = \rho(\omega R)^2/2$ – velocity head, Pa
 T – rotor thrust, N
 M_k – torque, Nm
 $C_T = T/(qS)$ – coefficient of rotor thrust
 $m_k = M_k/(qSR)$ – torque coefficient
 $Re_{\omega} = \omega r b/\nu$ – Reynolds number of blade section
 p – pressure, Pa
 $C_p = (p - p_0)/q$ – pressure coefficient
 p_0 – restoration pressure, Pa

2. INTRODUCTION

At present, in connection with the development and design of new aerodynamic configurations of perspective high-speed helicopters, numerical methods for calculating the aerodynamic characteristics of the rotors are intensively developed and applied. The vortex models based on

non-linear vortex theory of rotating blade and successfully applied to the rotors in the modes of “vortex ring”, the axial and oblique flow, have long been developed and now are widely used for calculations. However, the vortex methods do not take into account the compressibility effects, viscous and separation phenomena caused by the rotation of the blades and specified for different blade sections. Numerical studies of these characteristics are usually carried out using methods of computational fluid dynamics (CFD), based on the grid methods for solving the Navier-Stokes and Reynolds equations (RANS, URANS methods). These methods are being implemented in the various copyright, scientific and commercial CFD software systems, which are intensively developing together with the rapid growth of computing capacities of computers, supercomputers and clustered systems.

In the first part of the paper we present the results of the verification and validation of the numerical methods used by the author. In order to test the new codes there have been developed the methodologies of calculation of flow around rotor in two CFD software complexes, commercial code ANSYS CFX [1] and the new Russian package LOGOS [2], based on the grid methods of solution of the averaged Navier-Stokes equations (RANS, URANS). Series of methodical and systematic calculations have been performed to determine the effect of topology and size of the computational domain, the type of boundary conditions and other parameters. In order to test computer codes CFX and LOGOS and to verify the numerical results with experimental data, comparative calculations of

three-dimensional flow model of the rotating two-bladed helicopter rotor have been carried out. A good agreement between the results of calculations of integral and distributed characteristics of two-carried bladed rotor in hover with the data of experiment [3], carried according to standard procedure of TSAGI.

In urgent task at present the study of flow around helicopter airfoils shaping the high speed helicopter rotor blades rotating with the rate of a few revolutions per second, computational methods of nonstationary aerodynamics come forward. The principal objective is to create a data bank of stationary and nonstationary aerodynamic characteristics of helicopter airfoils developed on the basis of numerical algorithms and computational technologies. Further difficulties lie in the fact that experimental studies in wind tunnels and the measurement of unsteady aerodynamic characteristics of helicopter airfoils in the incoming flow with the high-frequency oscillations of the speed in the transonic range, as well as test stand modeling back-and-forth movement of an airfoil with a high frequency in the direction of incident flow are not currently possible.

In the second part of the paper the results of calculations of nonstationary aerodynamic characteristics of helicopter NACA 23012 airfoil and NACA 0012 symmetric airfoil in the transonic range of free-stream Mach number $M=0.3\div 0.9$ are discussed. There has been developed the technology of calculating airfoil characteristics in the oscillating flow with a given periodic changes of incoming flow velocity by time. Calculations of two-dimensional nonstationary airfoil flow in this formulation require the use of very high quality mesh, sufficiently small time integration step (10^{-5} - 10^{-4} s or less) and computing clusters for tasks parallelization. As a result of numerical research and calculations of nonstationary aerodynamic characteristics of airfoils there has been revealed the phenomenon of formation of the hysteresis loop of airfoil lift and drag against the free stream Mach number decrease and increase.

The third part of the paper describes the possibilities and prospects of other approaches and numerical methods to solve this class of problems for rotary-wing aircraft differing in the presence of rotating elements and the nonstationary nature of the flow. This category of methods includes relatively new developing code XFlow [4] designed by Next Limit Technologies (Spain). XFlow software package is based on the meshless Lagrangian particles technology for solving Boltzmann equations with the LES models of turbulence in the framework of the lattice Boltzmann equations LBM method (Lattice Boltzmann Method). As an illustration of the method, the results of calculations of separated

subsonic flow around an airfoil NREL S809 at large angle of attack are presented

3. CFD CALCULATIONS OF FLOW AROUND THREE-DIMENSIONAL MODEL OF HELICOPTER MAIN ROTOR

The CFD technique of calculation of three-dimensional flow model of the rotating helicopter main rotor has been worked out. There are presented the results of verification and validation of two CFD software systems ANSYS CFX [1] and LOGOS [2], used by the author and based on the grid methods of solution of the averaged Navier-Stokes equations (RANS, URANS). In order to test computer codes CFX and LOGOS and to verify the numerical results with experimental data there have been carried out comparative calculations of flow around a three-dimensional model of a rotating two-bladed rotor. Calculations of aerodynamic characteristics of the model of two-bladed helicopter rotor in hover with different non-zero angles of blade incidence have been made; the dependence of the rotor thrust coefficient c_t versus the coefficient of torque c_m (c_t (c_m) polar) in hover has been obtained. The results obtained were compared with experimental data [3]. The comparison of the calculated pressure distributions in the two sections of the rotor blade with the experimental diagrams of pressure [3] has been run.

3.1. Geometry

Mathematical model of geometry used for the calculations consists of two rectangular shaped rotating blades of the rotor. The geometry of the model corresponds to the paper [3]. The shaft and the tool holders in the calculation have not been modeled.

View of the computational model is shown in Figure 1. Calculations were carried out in the aerodynamic experiment conditions [3], so the size of the design geometry matched the size of the experimental model. Parameters and geometrical dimensions of the model are shown in Table 1.

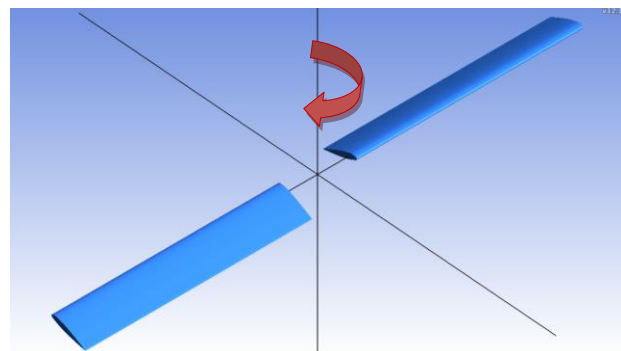




Figure 1. Geometry of the computational model and NACA 23012 airfoil profile in the section of the blade

Table 1. Parameters of the calculation model

rotor radius	1 m
radius of blade root	0.12 m
blade chord	0.15 m
number of blades	2
filling factor	0.0956
angle of incidence of the blade	0, 3°, 6°, 9°, 12°, 15°, 18°
number of rotor revolutions per minute	545 rev/min (polar) 500 rev/min (pressure in blade sections)
blade airfoil	NACA 23015

3.2. Grid

For each angle of incidence of rotor blade there was generated unstructured mesh with a high degree of space discretization in the vicinity of the surface of the blade and in the regions of the formation of vortices coming down from the blade-tip and blade-root in hover.

Figure 2 shows a fragment of a triangular mesh design on the surface of the blade model.

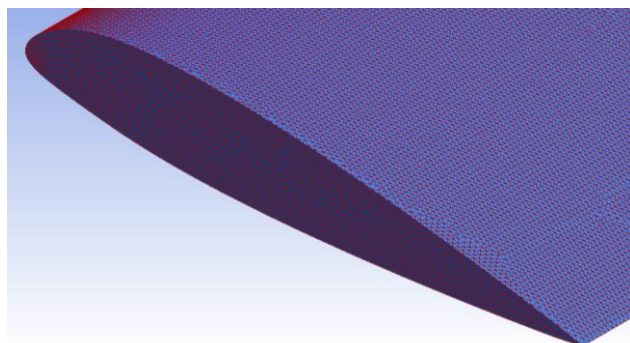


Figure 2. Fragment of a triangular mesh on the surface of the blade model

Three-dimensional volume grids contained about 1.5 million cells (coarse mesh), 5 million cells (middle mesh) and 12 million cells (fine mesh) respectively, which allowed sufficient in detail to calculate the structure of tip vortices (Figure 3) and the vortex sheet coming down from the side and trailing edges of the blades.

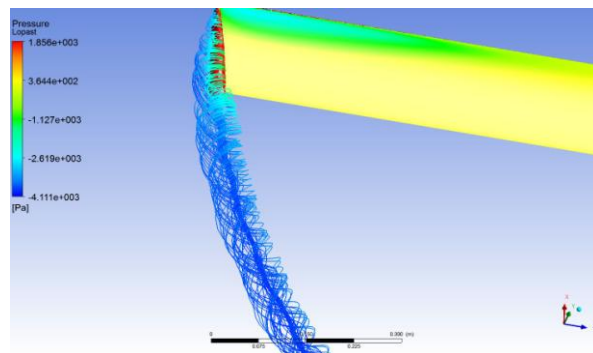


Figure 3. Visualization of blade-tip vortex structure

3.3. Calculation results

The problem of calculating the flow and aerodynamic characteristics of a rotating helicopter rotor was solved in a stationary statement with the use of a rotary blade coordinate system. Stationary Reynolds equations (RANS) for the model of a viscous compressible gas were solved numerically. Two-equation SST $k-\omega$ turbulence model with automatic wall functions was used for closing the motion equations. Boundary layer was calculated as fully turbulent.

In calculations the convergence of solution on the base of the behavior of the residuals of key variables of the problem and the integral characteristics against of the iteration number was analyzed. For the stationary problem the reduction of residual level by 3-5 orders was reached over 150-250 iterations (CFX code) or 500-700 iterations (LOGOS code). At the same time, the solution was considered as converged when the average value of the integral values (rotor thrust and torque) ceased to vary within a specified accuracy level.

Figure 4 shows the dependence of the rotor thrust coefficient c_t versus the coefficient of torque c_m in hover ($c_t(c_m)$ rotor polar).

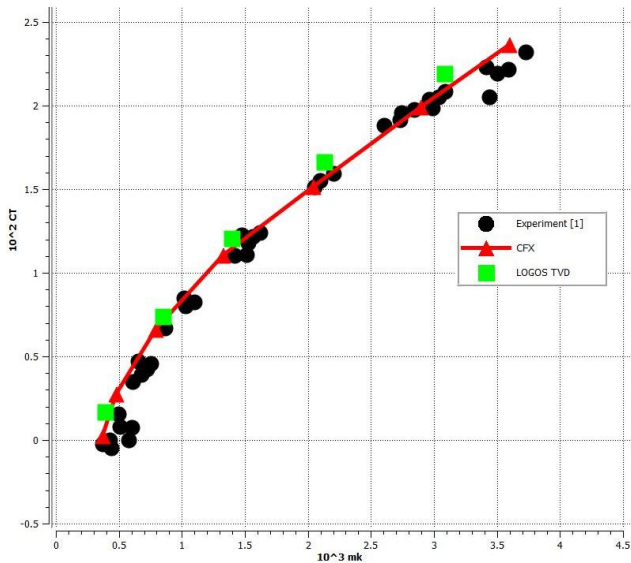


Figure 4. The dependence of the rotor thrust coefficient c_t versus the coefficient of torque c_m in hover; black markers - the experimental data [3], green markers - calculation in the LOGOS package, red markers - calculation in the CFX package

The comparison of the experimental [3] and calculated pressure coefficient diagrams in two sections along the span of the blade ($r/R = 0.24$ and 0.74). Scheme of blade control sections is shown in Figure 5.

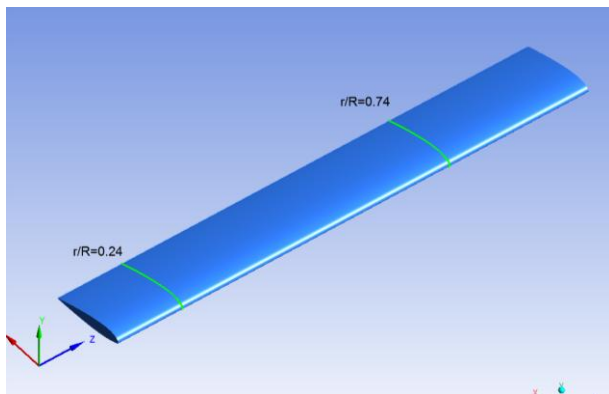


Figure 5. Scheme of blade control sections in which pressure coefficients were measured

Figures 6-7 show a comparison of the pressure coefficient diagrams in the calculation and experiment for the cross section $r/R = 0.24$ and the angles of blade incidence $\varphi=9^\circ$ and 18° , Figures 8-9 – for the cross section $r/R=0.74$ and the angles of incidence $\varphi=15^\circ$ and 18° respectively.

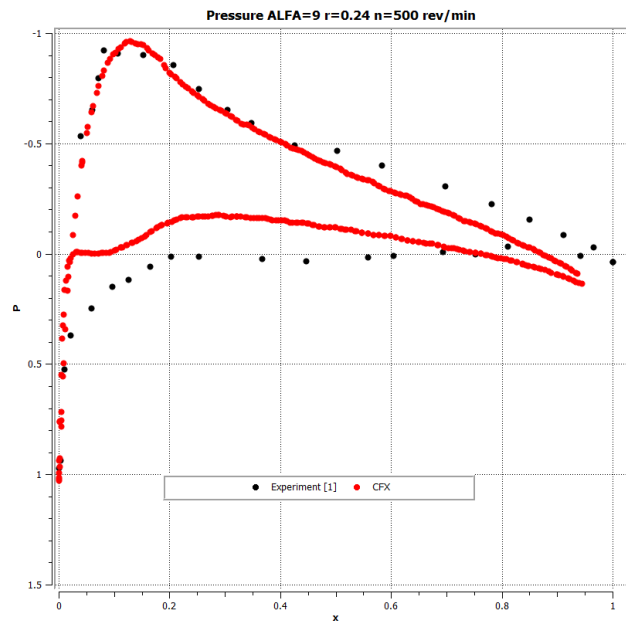


Figure 6. Pressure coefficient diagram in the blade root section; $r/R=0.24$, $Re_\omega=0.123 \cdot 10^6$, $\varphi=9^\circ$; black markers - the experimental data [3], red markers - calculation in the CFX package

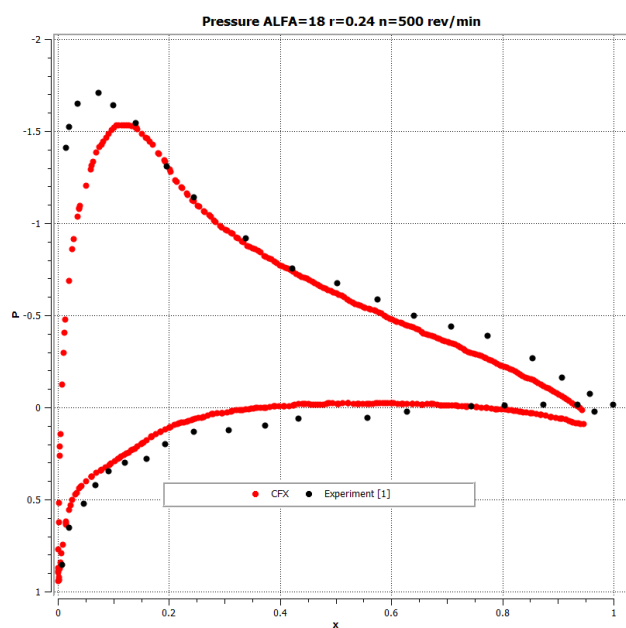


Figure 7. Pressure coefficient diagram in the blade root section; $r/R=0.24$, $Re_\omega=0.123 \cdot 10^6$, $\varphi=18^\circ$; black markers - the experimental data [3], red markers - calculation in the CFX package

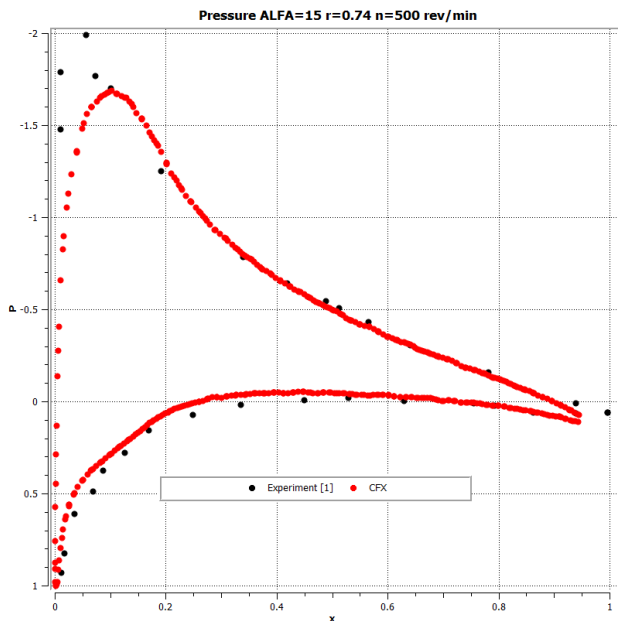


Figure 8. Pressure coefficient diagram in the blade tip section; $r/R=0.74$, $Re_{\omega}=0.4 \cdot 10^6$, $\varphi=15^\circ$; black markers - the experimental data [3], red markers - calculation in the CFX package

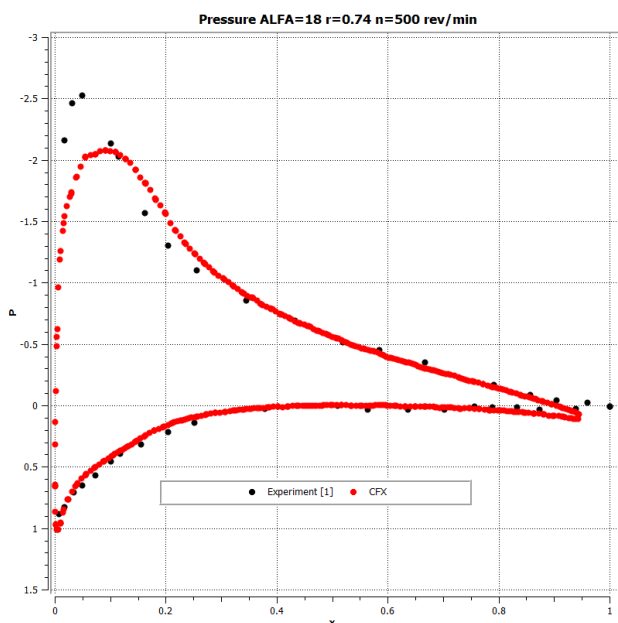


Figure 9. Pressure coefficient diagram in the blade tip section; $r/R=0.74$, $Re_{\omega}=0.4 \cdot 10^6$, $\varphi=18^\circ$; black markers - the experimental data [3], red markers - calculation in the CFX package

As can be seen from Figures 4, 6-9, there is a sufficiently good stable agreement between the experimental and numerical results of integral and distributed aerodynamic characteristics of a three-dimensional model of a rotating two-blade rotor in hover.

4. CFD CALCULATIONS OF NONSTATIONARY AIRFOIL FLOW

The results of calculations of nonstationary aerodynamic characteristics of the helicopter NACA 23012 and NACA 0012 symmetric airfoils in two-dimensional transonic flow in the range of free-stream Mach number $M=0.3 \div 0.9$ are discussed.

In order to simulate the features of unsteady flow of blade cross sections of high speed helicopter there is considered the airfoil flow with a given periodic law changes of the incident flow velocity from time to time:

$$(1) \quad V=V_0+\Delta V \cdot \sin(2\pi n t),$$

where $V_0=200$ m/s – “average” velocity, $\Delta V=100$ m/s – velocity amplitude, $n=5$ rev/s – rotation frequency of rotor blades (period of rotation 0.2 s), t – time in seconds.

All calculations were performed in two-dimensional setting in the ANSYS CFX software package. Unsteady Reynolds-averaged Navier-Stokes equations (URANS with SST $k-\omega$ turbulence model) describing the subsonic, transonic, and supersonic flows of viscous compressible gas without and with separation were solved. There have been made special methodical calculations in order to select and determine the most appropriate parameters of calculation method and optimum solver control (the topology and size of the design domain and grids, the input and output parameters, the key parameters of the numerical schemes and turbulence, etc.).

Analysis of the results of the methodical calculations has allowed identifying the “working” range of options for mass calculations of steady and unsteady flow and aerodynamic characteristics of the various helicopter airfoils with reasonable accuracy in order to create a data bank of their aerodynamic characteristics.

As shown by the numerical study calculations of the two-dimensional unsteady flow around an airfoil in such statement require the use of high quality grids, small enough time steps for integrating the equations of motion (10^{-5} - 10^{-4} s or less) and computer clusters for paralleling tasks.

Numerical research and analysis of aerodynamic characteristics of airfoils in the nonstationary periodic flow allowed revealing the phenomenon of formation of the hysteresis loop of airfoil lift and drag against the free stream Mach number.

4.1. Analysis of results for NACA 23012 airfoil

Calculations of nonstationary sinusoidal time-running flow around an airfoil NACA 23012 (Figure 10) in accordance with the statement (1) showed significant differences in the nature of the flow “before” and “after” the passage of a maximum flow

velocity equal to 300 m/s ($M=0.87$) corresponding to the point in time $t=0.05$ s (1/4 part of the oscillation period). Figures 11-13 show the calculation distributions of Mach numbers about an airfoil in steady flow (Figure 11, the free-stream Mach number $M=0.85$) and the nonstationary flow at times $t=0.04$ s and $t=0.06$ s (Figures 12-13), to that according to formula (1) the same incident flow Mach number $M=0.85$ corresponds. Flow patterns at time $t=0.04$ s and 0.06 s differ essentially in the position and intensity of shocks and separated zones on the upper and lower airfoil surface.



Figure 10. NACA 23012 airfoil profile

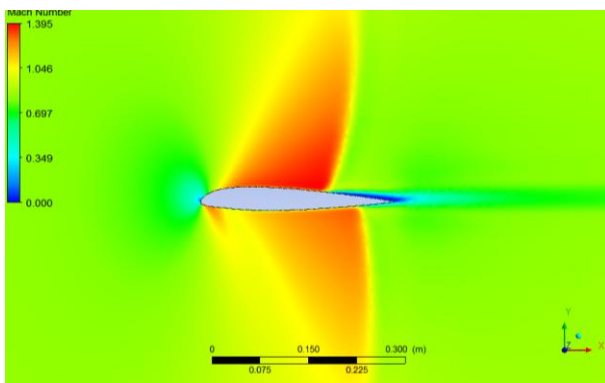


Figure 11. Calculated field of Mach numbers. Stationary flow, $M = 0.85$, $\alpha = 0^\circ$

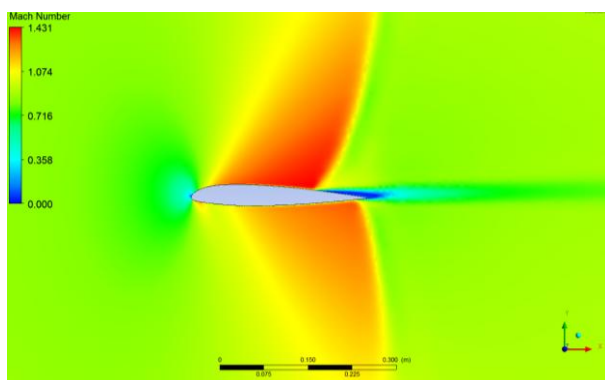


Figure 12. Calculated field of Mach numbers. Nonstationary flow (1), $M=0.85$, $\alpha=0^\circ$, time station $t=0.04$ s.

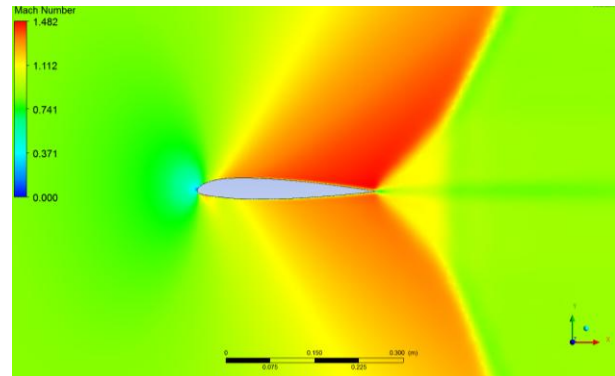


Figure 13. Calculated field of Mach numbers. Nonstationary flow (1), $M=0.85$, $\alpha=0^\circ$, time station $t=0.06$ s

4.2. Analysis of results for NACA 0012 airfoil

Calculations of nonstationary aerodynamic characteristics of NACA 0012 symmetric airfoil (Figure 14) have been performed for the purpose to research the possibility of application of CFD methods to calculate aerodynamic characteristics of airfoils in dynamic change of free-stream Mach number.



Figure 14. NACA 0012 airfoil profile

In the formulation (1) we consider the nonstationary flow about NACA 0012 airfoil in the periodic flow with sinusoidal time alternating the free-stream Mach number. Objective difficulties are that currently, it is not possible to conduct experimental studies of this nonstationary flow around an airfoil in a wide range of transonic free-stream Mach number $M=0.3 \div 0.9$. We know only one paper [5] with the results of experimental studies in the wind tunnel of unsteady oscillatory on velocity flow around NREL S805 airfoil, but only in a narrow range of subsonic speeds $M=0.35 \div 0.5$.

Calculations of nonstationary flow in the framework of formulation have revealed the phenomenon of aerodynamic characteristics hysteresis for NACA 0012 airfoil on the stream velocity, which manifests itself in different values of airfoil lift and drag coefficients in the "forward" and "reverse" motion on the free stream Mach number at its periodic change with sinusoidal law (Figures 15–16).

A similar hysteresis phenomenon of lift and moment coefficients against an incident flow with Mach number oscillations in a narrow subsonic range $M=0.35\div 0.5$ observed experimentally for the NREL S805 airfoil in [5].

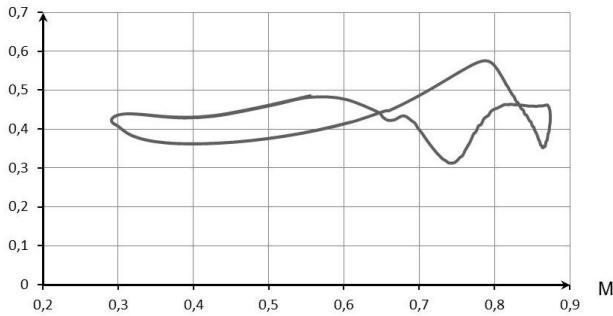


Figure 15. NACA 0012 airfoil lift hysteresis against free stream Mach number

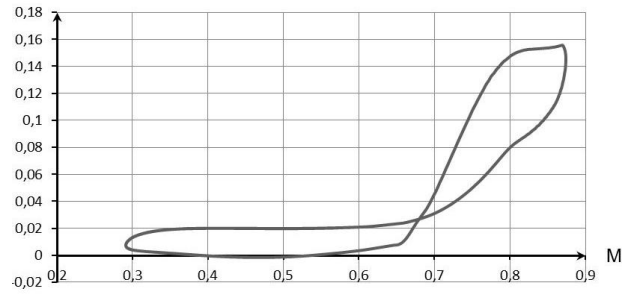
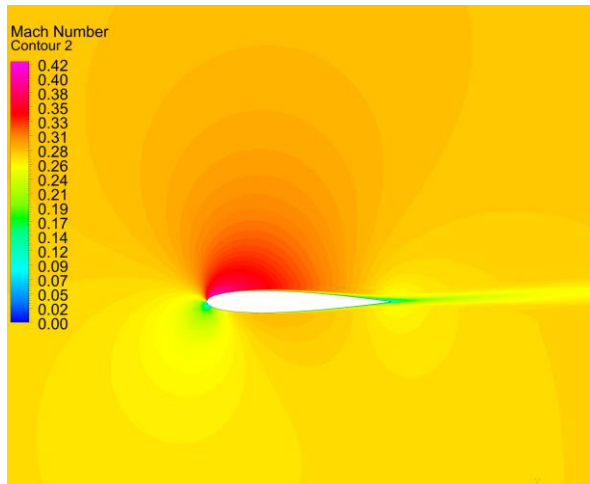


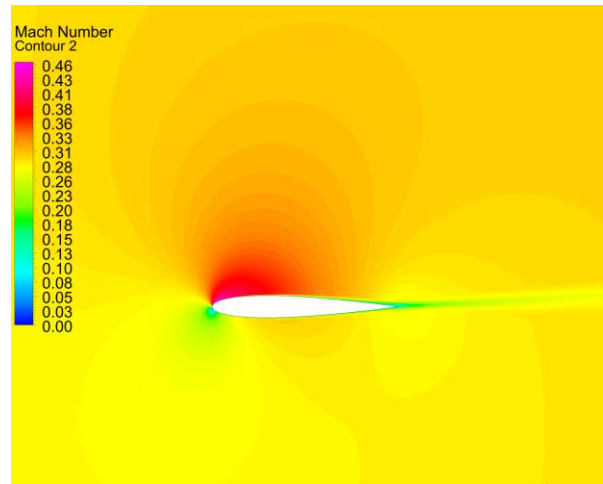
Figure 16. NACA 0012 airfoil drag hysteresis against free stream Mach number

The observed phenomenon of airfoil aerodynamic forces hysteresis is clearly accounted to the different nature of the flow around NACA 0012 airfoil in the "forward" and "back" strokes during the oscillation cycle of periodic free-stream Mach numbers (Figure 17).

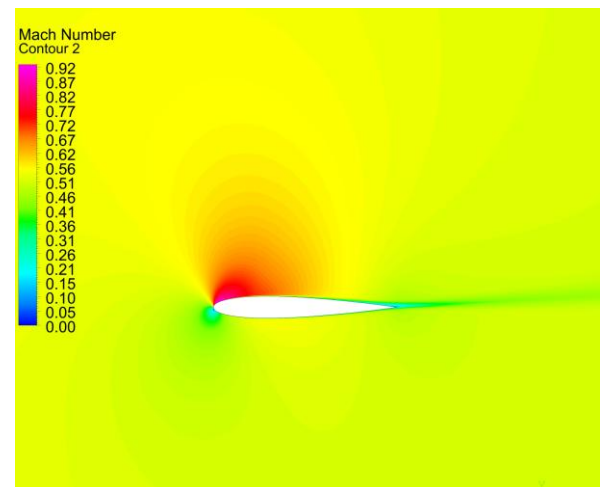
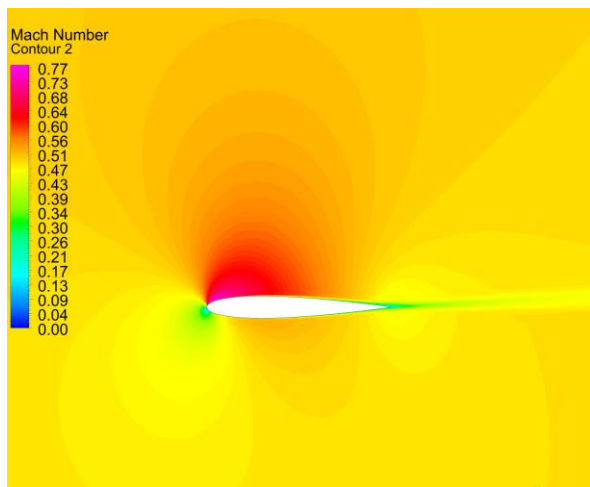
Increasing Mach number ("forward" stroke)



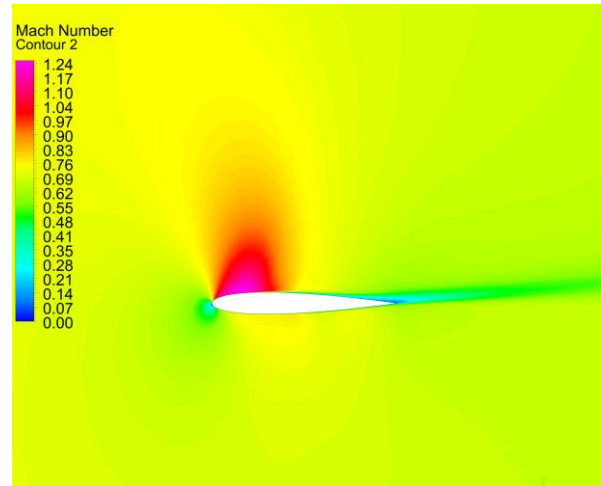
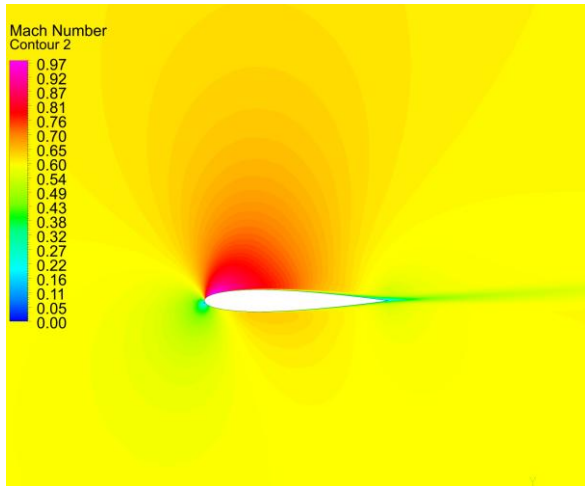
Decreasing Mach number ("back" stroke)



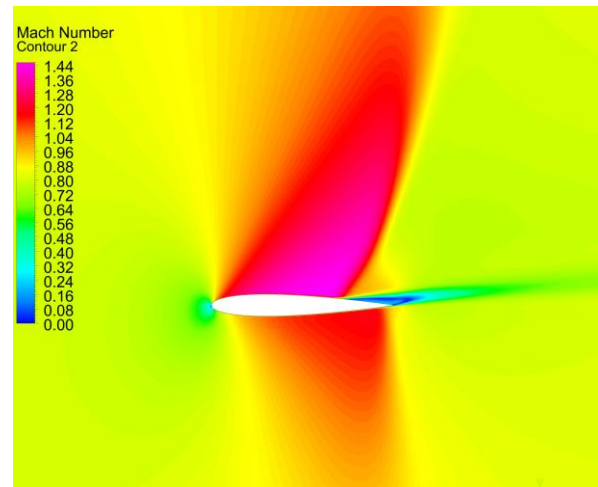
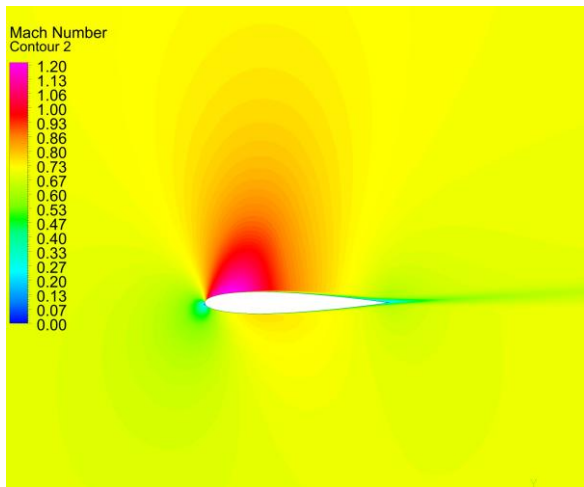
M=0.3



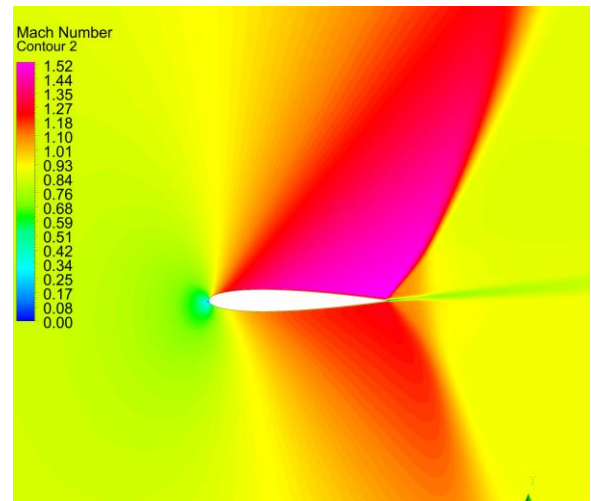
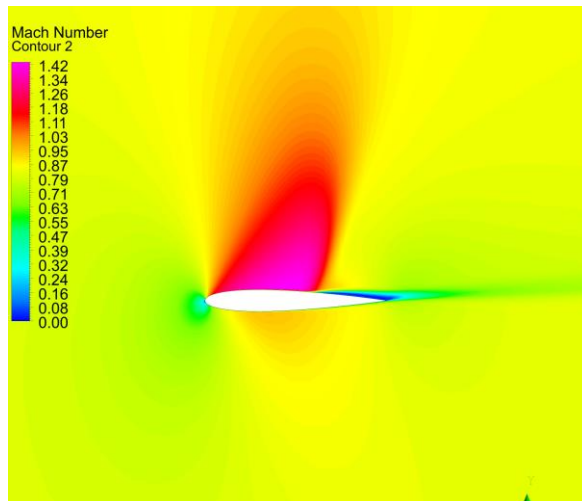
M=0.5



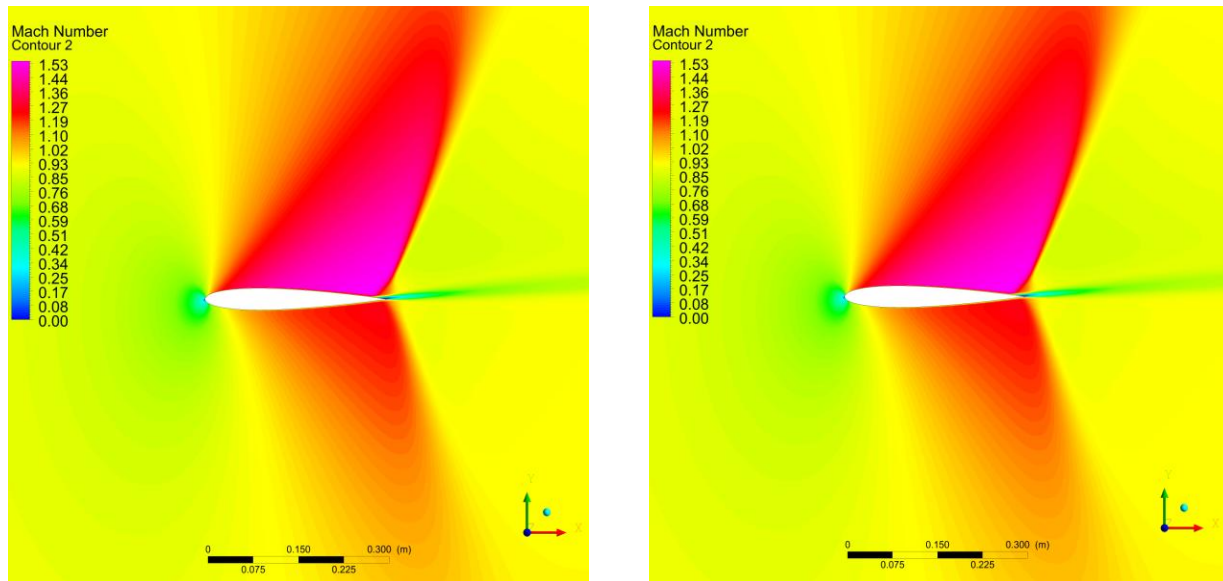
M=0.6



M=0.7



M=0.8



M=0.87

Figure 17. Transformation of Mach number field around NACA 0012 airfoil within the oscillation cycle (1) for flow velocity, angle of attack $\alpha = 4^\circ$.

5. XFLOW SOFTWARE PACKAGE FOR PROBLEMS OF NONSTATIONARY AERODYNAMICS

Software package XFlow [4] of Next Limit Technologies (Spain) is designed to simulate unsteady flows of viscous heat-conducting liquids and gases. Numerical Lattice Boltzmann Method (LBM) is used for solving lattice Boltzmann equations. Large Eddy Simulation (LES) technologies are used for turbulence simulation. Methodology of XFlow code, based on the interaction of Lagrangian fluid particles in cells allows relative easy simulating unsteady flows and solving numerically various flow tasks with moving and rotating elements and boundary conditions. Rotary-wing aircraft and helicopters get naturally into this class of problems (Figures 18-19).

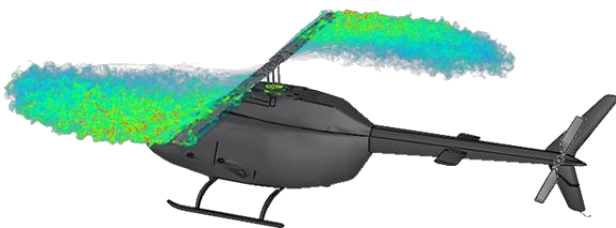


Figure 18. XFlow calculation (picture from the website www.xflowcf.com)



Figure 19. XFlow calculation (picture from the website www.xflowcf.com)

Usually, to solve problems of fluid flow and heat and mass transfer, CFD methods based on the numerical solution of the Navier-Stokes and Reynolds equations are applied. In the last 20 years there is actively developed an alternative approach in which the discretized Boltzmann kinetic equation for the evolution of distribution function is solved to simulate viscous fluid flows. The essence of the method lies in the fact that the investigated flow region is divided into a finite number of square or cubic cells with liquid particles, between which each time step the mass transfer takes place in

accordance with a predetermined form of the kinetic equation and the collision integral.

LBM method has now reached a high level of development and its capabilities are comparable or exceed the capabilities of traditional methods for solving the Navier-Stokes equations. LBM method is time-dependent, time-explicit method and it is naturally parallelized by a large number of cores (Figure 20) and allows using graphics processors. Efficiency and acceleration of computation can reach hundreds of times over the algorithms based on the solution of the Navier-Stokes equations by finite volume methods.

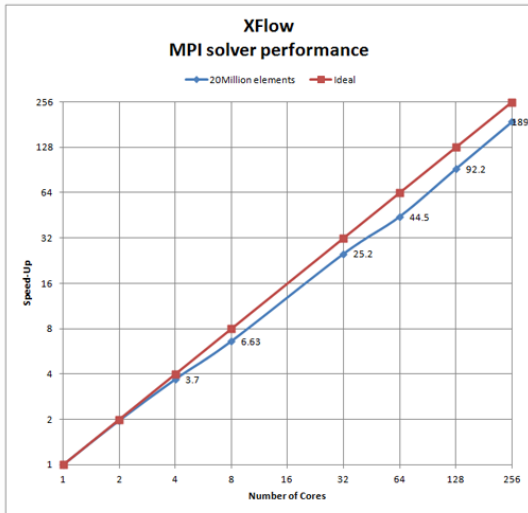


Figure 20. The effectiveness of parallelization of XFlow code (from the website www.xflowcf.com)

Lattice Boltzmann method describes well the dynamics of liquids and gases for a wide class of problems and it is consistent with the Navier-Stokes equations: Chapman-Enskog method (S. Chapman, 1916; D. Enskog, 1917) allows proving that the behavior of the medium described by the Boltzmann equation with a certain collision operator conforms to the Navier-Stokes equations.

5.1. Summary of fundamentals of the lattice Boltzmann method

The computational domain is divided into uniform square (in two dimensions) or cubic (in three dimensions) cells. The particles of matter from the cell nodes can move only to neighboring nodes via dedicated directions. There are used lattice stencils that provide sufficient accuracy and stability of calculations of the evolution of the system in range of parameters under consideration. These are the D2Q9 lattice with 9 velocities in two-dimensional space and the D3Q19 with 19 velocities in three dimensions (Figure 21).

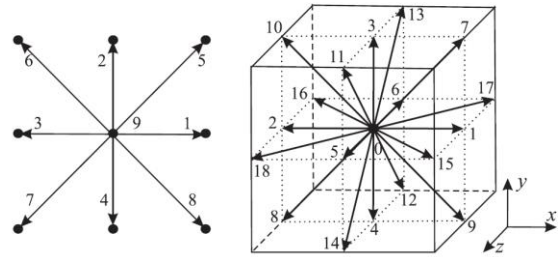


Figure 21. Two-dimensional D2Q9 lattice (left) and three-dimensional D3Q19 lattice (right)

The lattice Boltzmann equation can be written as:

$$f_a(x + e_a \delta t, t + \delta t) = f_a(x, t) + \Omega_a(x, t),$$

where f_a – one-particle distribution function for the selected discrete direction a , e_a - discrete velocity, δt - time step, $\Omega_a(x, t)$ - collision integral. Macroscopic parameters of density ρ and the average velocity u are calculated as the first principal moments of the one-particle distribution function as follows:

$$\rho = \sum_a f_a \quad \rho u = \sum_a e_a f_a$$

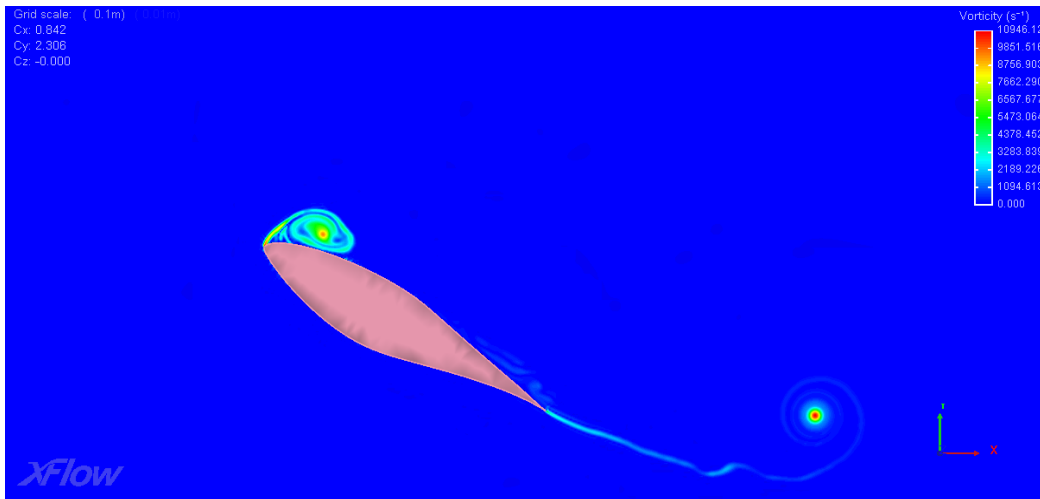
To describe the motion of gas in LBM methods collision integral is used as BGK (Bhatnagar - Gross - Krook) approximation, which is a linear relaxation of the system to local equilibrium:

$$\Omega_a = \frac{1}{\tau} (f_a^{eq} - f_a)$$

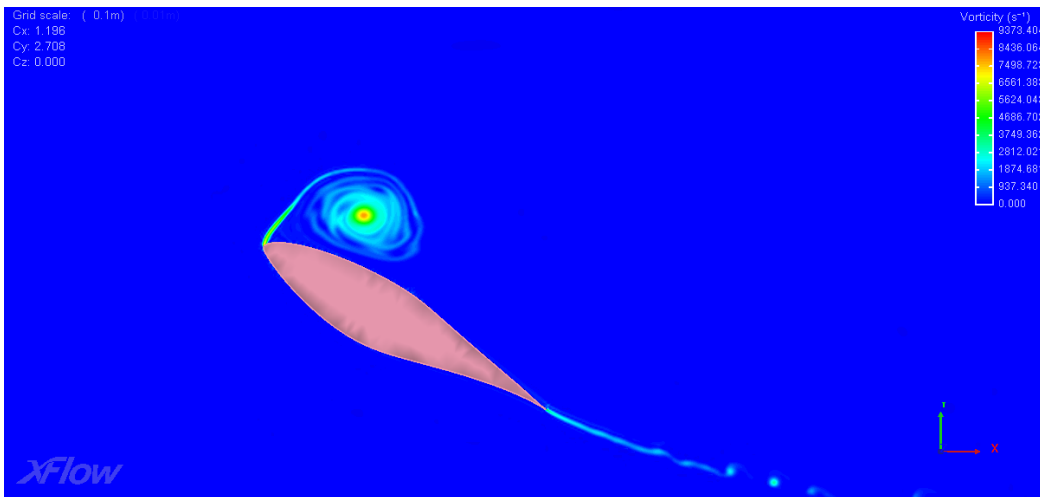
where f_a^{eq} - equilibrium one-particle distribution function and τ - dimensionless relaxation parameter. It is assumed in the model that in each local domain particles obey the Maxwell-Boltzmann distribution

5.2. Visualization of the calculation results of airfoil detached flow in the XFlow software package

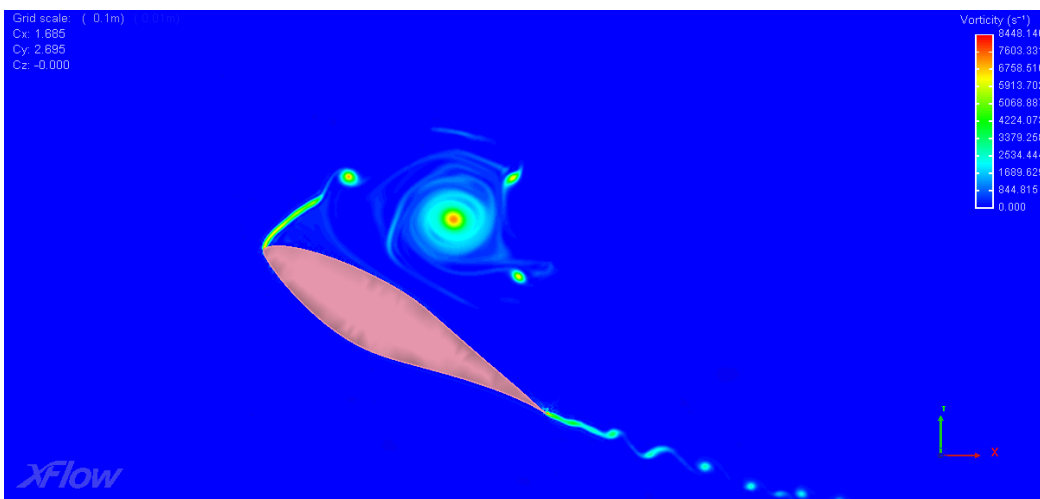
To illustrate the specific features and performance capabilities of XFlow code the author calculated the flow around NREL S809 airfoil at large angle of attack $\alpha=30^\circ$ by subsonic viscous stream with Mach number $M=0.15$ at Reynolds number $Re=500\,000$. Unsteady developed separated flow around this airfoil corresponds to specified parameters. Figure 22 shows the flow frames in consecutive order (visualization of the vorticity field) at different time points of flow progress around an airfoil, with time interval equal to 0.02 s. On the fragments we can clearly see the dynamics of formation of separated bubble on the upper surface of airfoil forepart, its subsequent separation, distortion, destruction and transfer downstream. Also the calculation shows the formation of tip vortex at the trailing edge of the airfoil, its subsequent detachment and transfer.



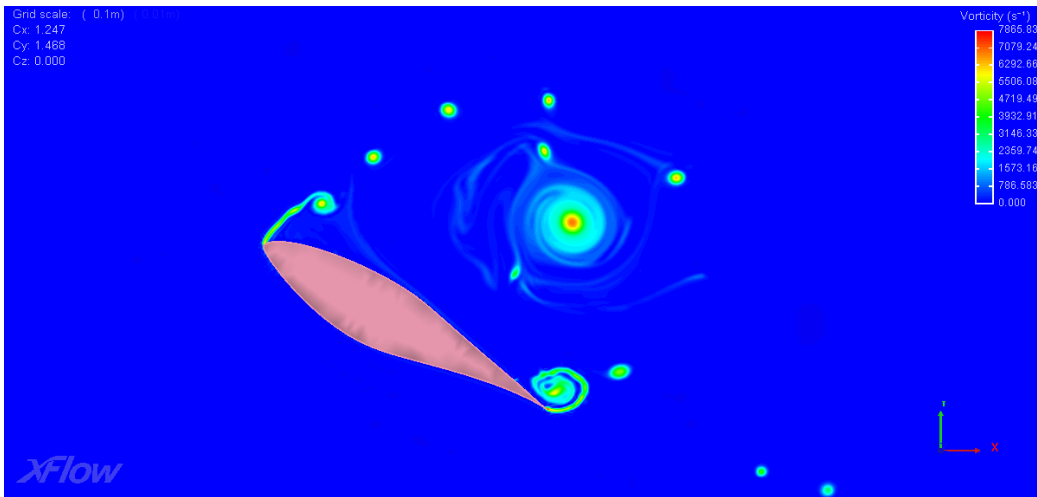
Time point $t=0.02$ s



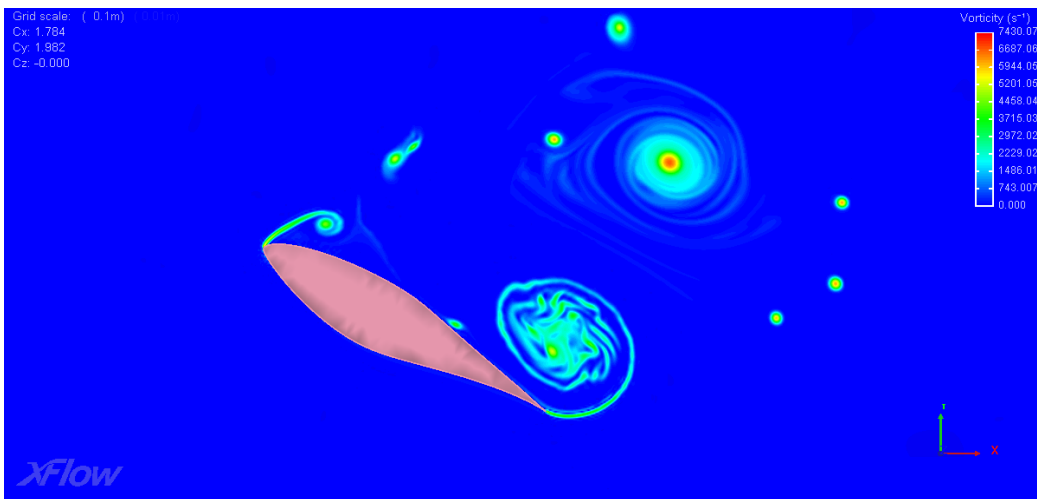
Time point $t=0.04$ s



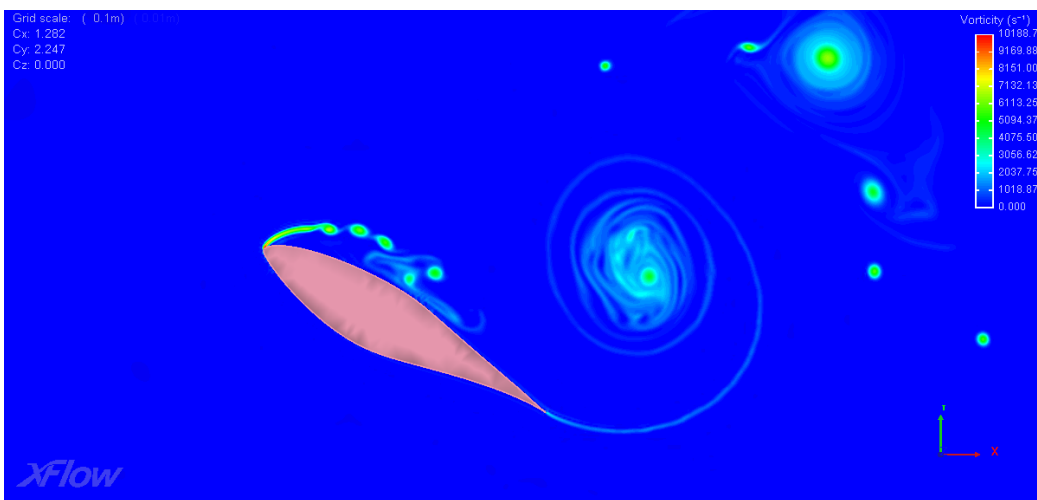
Time point $t=0.06$ s



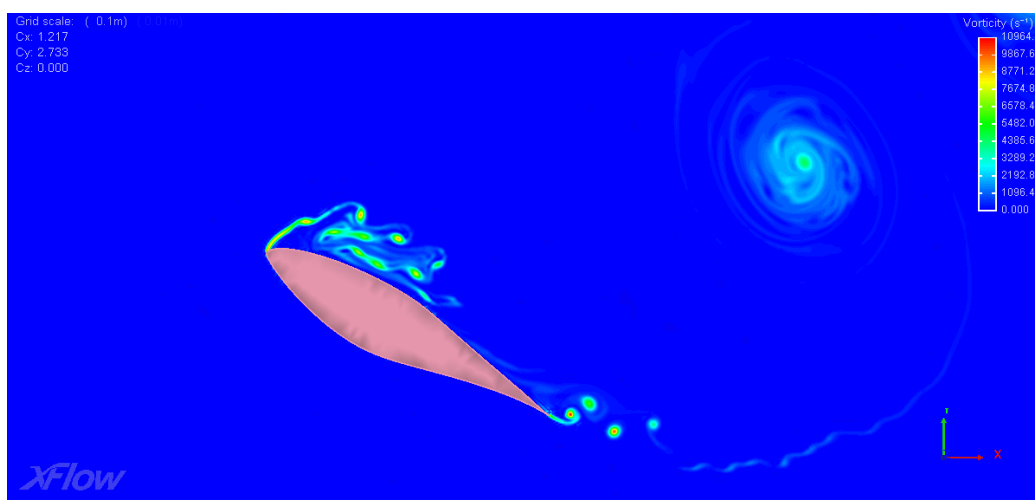
Time point $t=0.08$ s



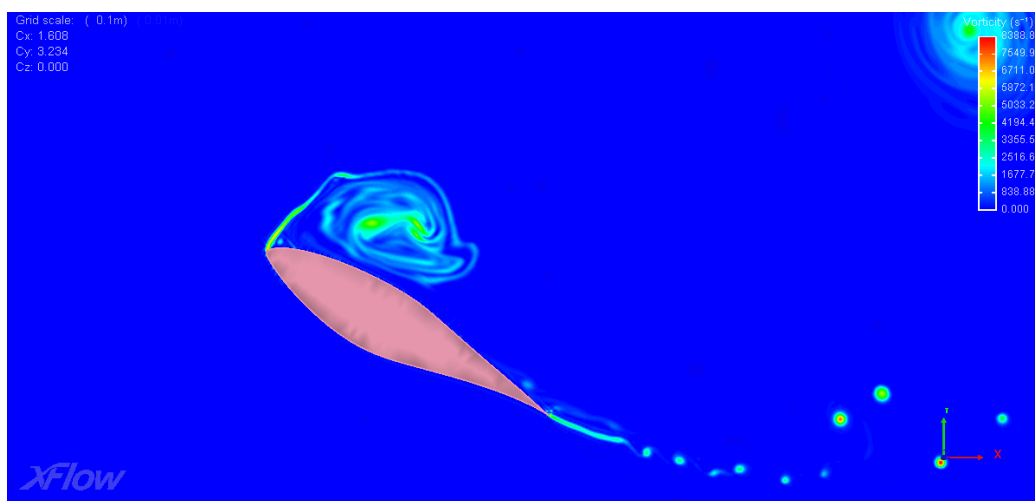
Time point $t=0.10$ s



Time point $t=0.12$ s



Time point t=0.14 s



Time point t=0.16 s

Figure 22. Vorticity field near NREL S809 airfoil, $M=0.15$, $\alpha=30^\circ$, $Re = 500\,000$. Unsteady separated flow at different points in time. The calculation in the XFlow package.

6. CONCLUDING REMARKS

The results of the author's calculations and tests in order to simulate flow characteristics of rotating helicopter rotor and helicopter airfoils, forming high-speed helicopter blade, showed the availability of the use and relatively high accuracy of state-of-the-art methods of computational aerodynamics and CFD software packages ANSYS CFX, LOGOS, XFlow.

The results of verification and validation of numerical codes have shown good agreement between the calculated and experimental data for integrated and distributed aerodynamic characteristics of three-dimensional model of two-bladed rotor in hover.

Numerical studies of nonstationary oscillating flow around helicopter airfoils have revealed lift and drag hysteresis in the transonic range of free-stream Mach numbers.

The results obtained may serve as a basis for the generation of data bank of stationary and non-stationary aerodynamic characteristics of helicopter airfoils and rotors by force of CFD technologies application.

Work towards improving and increasing the accuracy of the numerical methods, the development of new algorithms and techniques of the calculations to model more complex helicopter configurations should be undoubtedly supported and continued.

Acknowledgements

The author is grateful to colleagues from JSC "Kamov" for useful discussions and MSC Software Corporation, partner of Next Limit Technologies in 2011-2012, for provision of XFlow code test license.

References

- [1] ANSYS CFD user's manual, Release 14.0 // ANSYS, Inc. November 2011.
- [2] LOGOS Software Package. Technical manual. Version 4.0.1 // Federal State Unitary Enterprise (FSUE) "RFNC – VNIIEF", September 2012 (in Russian).
- [3] Pavlov A.S. Investigation of main rotor blades flow // Trudy TsAGI, vol. 1287, 1971 (in Russian).
- [4] XFlow 2012 User Guide // © 2012 Next Limit Technologies.
- [5] Kyle A. Gompertz, Christopher D. Jensen, James W. Gregory, and Jeffrey P. Bons Compressible Dynamic Stall Mechanisms Due to Airfoil Pitching and Freestream Mach Oscillations // American Helicopter Society 68th Annual Forum, Fort Worth, Texas, May 1-3, 2012.

Copyright Statement

The authors confirm that they, and/or their company or organization, hold copyright on all of the original material included in this paper. The authors also confirm that they have obtained permission, from the copyright holder of any third party material included in this paper, to publish it as part of their paper. The authors confirm that they give permission, or have obtained permission from the copyright holder of this paper, for the publication and distribution of this paper as part of the ERF2013 proceedings or as individual offprints from the proceedings and for inclusion in a freely accessible web-based repository.